Vol 18 No 12, December 2009
1674-1056/2009/18(12)/5375-10

Chinese Physics B

© 2009 Chin. Phys. Soc.
and IOP Publishing Ltd

Optimization control of modulation-instability gain in photonic crystal fibres with two zero-dispersion wavelengths*

Wang He-Lin(王河林)†, Leng Yu-Xin(冷雨欣), and Xu Zhi-Zhan(徐至展)

State Key Laboratory of High Field Laser Physics, Shanghai Institute of Optics and Fine Mechanics, Chinese Academy of Sciences, Shanghai 201800, *China*

(Received 4 January 2009; revised manuscript received 7 May 2009)

We design three kinds of photonic crystal fibres (PCF) with two zero-dispersion wavelengths (ZDWs) using the improved full vector index method (FVIM) and finite-difference frequency domain (FDFD) techniques. Based on these designed fibres, the effect of fibre structure, pump power and wavelength on the modulation instability (MI) gain in the anomalous dispersion region close to the second ZDW of the PCFs is comprehensively analysed in this paper. The analytical results show that an optimal MI gain can be obtained when the optimal pump wavelength (1530 nm) is slightly shorter than the second ZDW (1538 nm) and the optimal pump power is 250 W. Importantly, the total MI gain bandwidth has been increased to 260 nm for the first time, so far as we know, for an optimally-designed fibre with $\Lambda = 1.4$ nm and $d/\Lambda = 0.676$, and the gain profile became much smoother. The optimal pump wavelength relies on the second ZDW of the PCF whereas the optimal pump power depends on the corporate operation of the optimal fibre structure and optimal pump wavelength, which is important in designing the most appropriate PCF to attain higher broadband and gain amplification.

Keywords: modulation instability gain, broadband amplification, optimization control

PACC: 4281W, 4265K

1. Introduction

As a special four-wave mixing (FWM) process, modulation instability (MI) has attracted much attention for supercontinuum (SC) generation and broadband amplification in recent experimental investigations.[1−3] Due to an interplay between nonlinear and dispersive effects, MI occurs and manifests itself as the breakup of a CW or quasi-CW into a train of ultra-short pulses.[4] In general, MI appears in the anomalous group velocity dispersion (GVD) regime.[5] However, MI may occur in the normal GVD regime in some special cases, such as in the presence of higher even-order linear dispersions,[6] or the co-propagation of two or more optical fields in the optical fibre.[7]

Many authors have studied MI in optical fibres,[8−12] including photonic crystal fibres (PCFs).[13] However, the practical application of MI is extensive. For example, as a combination of parametric and Raman gain, MI gain may be exploited as a relatively broadband and tunable gain mechanism in highly nonlinear fibre-based frequency converters[14,15] and oscillators.[16,17] Moreover, a general drawback of parametric amplification is that it is a narrowband gain mechanism that requires sideband detuning close to the phase-matching condition, unless multiple frequency pump schemes are employed. Therefore, as a promising technique for providing broadband amplification and wideband loss compensation in the fibre-optical transmission link, MI gain and control are worthwhile research fields.

In this work, beginning from the extensively accepted nonlinear Schrödinger equation, we deduce the general expression of the MI, which includes the corporate operation of parametric and Raman gain. By applying the improved full vector effective index method (FVEM) or finite-difference frequency domain (FDFD) techniques, we firstly design three kinds of PCFs with two ZDWs (their second ZDWs are the same and equal to $\lambda_{\rm ZDW} = 1538$ nm), and then discuss an interesting situation where their group velocity dispersions (GVD) β_2 are negative and the fourth-order dispersions (FODs) β_4 are positive for pump wavelengths slightly less than their second ZDWs, for instance, in an approximately 8 nm region (1530 nm) of

*Project supported by the National Key Basic Research Program of China (Grant No 2006CB806001), the Knowledge Innovation Program of the Chinese Academy of Sciences (Grant No KGCX-YW-417-2), and Shanghai Commission of Science and Technology, China (Grant No 07JC14055).

†Corresponding author. E-mail: whl982032@163.com

downshift from their second ZDWs (1538 nm). The research results show that high-order dispersion, pump wavelength and power have a great effect on MI gain bandwidth and profile, and the corporate operation of GVD and FOD can make the gain bandwidth increase to over 120 nm. Finally, as we will discuss in this paper, by optimizing the fibre structure parameters, pump wavelength and power, one can obtain an optimal broadband MI gain bandwidth of ∼130 nm and a flat-top gain profile at the anti-Stokes sideband or Stokes sideband for the first time. The total gain bandwidth on both sides of the optimal pump wavelength (1530 nm) is 260 nm.

2. Theoretical model

Without considering polarization coupling, the pulse propagation in fibres is described by the scalar nonlinear Schrödinger equation (NLSE). To describe all nonlinear phenomena such as dispersion, self-phase modulations (SPM), self-steepening (SS), stimulated Raman scattering (SRS) and four wave mixing (FWM), the NLSE has to be expressed as follows:

$$\frac{\partial U(z,t)}{\partial z}+\frac{\alpha}{2}U(z,t)+\left(\sum_{n\geq 2}\beta_n\frac{\mathrm{i}^{n-1}}{n!}\frac{\partial^n}{\partial t^n}\right)U(z,t)=\mathrm{i}\gamma\left(1+\frac{\mathrm{i}}{\omega_\mathrm{p}}\frac{\partial}{\partial t}\right)\left(U(z,t)\int_{-\infty}^{\infty}R(\tau)|U(z,t-\tau)|^2\mathrm{d}\tau\right), \quad (1)$$

where $U(z,t)$ is the electric field amplitude, z is the longitudinal coordinate along the fibre, t is the time in a reference frame travelling with the pump light ω_p, $\beta_n=\partial^n\beta(\omega)/\partial\omega^n|_{\omega=\omega_\mathrm{p}}$ is the n-th-order frequency dependence dispersion coefficient at the central frequency of the pump pulse, $\gamma=n_2\omega_\mathrm{p}/cA_\mathrm{eff}$ is the nonlinear parameter, $n_2=3.0\times10^{-20}$ m^2/W is the nonlinear refractive index of fused-silica glass, and A_eff is the effective mode area of the fibre which depends on fibre parameters such as the core radius and the core-cladding index difference; α is the fibre loss. In order to obtain an exact estimate of the effect of Raman gain, the Raman response function can be written in the form:[18]

$$R(t)=(1-f_\mathrm{R})\,\delta(t)+f_\mathrm{R}\left[(f_\mathrm{a}+f_\mathrm{c})\,h_\mathrm{a}(t)+f_\mathrm{b}h_\mathrm{b}(t)\right], \quad (2)$$

where

$$h_\mathrm{a}(t)=t_1(t_1^{-2}+t_2^{-2})\exp(-t/t_2)\sin(t/t_1),$$
$$h_\mathrm{b}(t)=\left[(2t_\mathrm{b}-t)/t_\mathrm{b}^2\right]\exp(-t/t_\mathrm{b})$$

with $t\geq 0$. Equation (2) includes both instantaneous electronic and delayed Raman contributions[18] and is much more exact than the traditional single-Lorentzian model; $f_\mathrm{R}=0.18$ is the fraction of the Raman contribution to the nonlinear polarization. $f_\mathrm{a}=0.75$, $f_\mathrm{b}=0.21$ and $f_\mathrm{c}=0.04$ represent the fractional contributions of the isotropic and anisotropic parts of the Raman response, respectively; $t_1=12.2$ fs, $t_2=32$ fs, $t_\mathrm{b}=96$ fs are the chosen parameters. By introducing the Fourier transform $\int_{-\infty}^{\infty}R(t)\exp(\mathrm{i}\Omega t)\,\mathrm{d}t=R(\Omega)$, in view of Eq.(2), we can obtain

$$R(\Omega)=(1-f_\mathrm{R})+\frac{f_\mathrm{R}\left(t_1^2+t_2^2\right)\left[t_1^2+t_2^2(1-t_1^2\Omega^2)\right](f_\mathrm{a}+f_\mathrm{c})}{\left[t_1^2+t_2^2(1-t_1\Omega)^2\right]\left[t_1^2+t_2^2(1+t_1\Omega)^2\right]}+\frac{\left(1+3t_\mathrm{b}^2\Omega^2\right)f_\mathrm{R}f_\mathrm{b}}{\left(1-t_\mathrm{b}^2\Omega^2\right)^2+(2t_\mathrm{b}\Omega)^2}$$
$$+\mathrm{i}\left[\frac{2t_1^2t_2f_\mathrm{R}\left(t_1^2+t_2^2\right)(f_\mathrm{a}+f_\mathrm{c})\,\Omega}{\left[t_1^2+t_2^2(1-t_1\Omega)^2\right]\left[t_1^2+t_2^2(1+t_1\Omega)^2\right]}+\frac{2t_\mathrm{b}^3f_\mathrm{R}f_\mathrm{b}\Omega^3}{\left(1-t_\mathrm{b}^2\Omega^2\right)^2+(2t_\mathrm{b}\Omega)^2}\right], \quad (3)$$

where $\Omega=\omega-\omega_\mathrm{p}$, ω is the actual optical frequency.

3. General expression for modulation-instability gain

By restricting our analysis to the undepleted-dump approximation, MI in the NLSE is revealed by a line stability analysis of its continuous wave (CW) pumped with a power P_p, whose evolution along the PCF reads

$$U(z)=\sqrt{P_\mathrm{p}}\exp\left[\mathrm{i}\gamma P_\mathrm{p}z\right]. \quad (4)$$

Equation (4) implies that CW light should be unchanged during propagation through the fibre except for acquiring a power-dependence phase shift.

To investigate the effect of small perturbations on the steady solution, we perturb the steady state slightly such that

$$\begin{aligned} U(z,t) = & \sqrt{P_{\mathrm{p}}}\exp\left[\mathrm{i}\gamma P_{\mathrm{p}} z\right] \\ & + u_{\mathrm{s}}(z)\exp(\mathrm{i}\Omega t)\exp\left[\mathrm{i}\gamma P_{\mathrm{p}} z\right] \\ & + u_{\mathrm{as}}(z)\exp(-\mathrm{i}\Omega t)\exp\left[\mathrm{i}\gamma P_{\mathrm{p}} z\right], \end{aligned} \quad (5)$$

where $u_{\mathrm{s}}(z)$ and $u_{\mathrm{as}}(z)$ are the small signal amplitudes of the Stokes and anti-Stokes waves at frequency shifts $\pm\Omega$, respectively, and here $\Omega = \omega_{\mathrm{p}} - \omega_{\mathrm{s}} = \omega_{\mathrm{as}} - \omega_{\mathrm{p}}$ ($\Omega > 0$). After inserting Eq.(5) into Eq.(1), two coupled linear ordinary differential equations are attained by picking out the Stokes term and the complex conjugate of the anti-Stokes term and making them linearized. They can be written as

$$\frac{\mathrm{d}}{\mathrm{d}z}\begin{pmatrix} u_{\mathrm{s}}(z) \\ u_{\mathrm{as}}^{*}(z) \end{pmatrix} = \mathrm{i}\begin{pmatrix} a_{11} & a_{12} \\ a_{21} & a_{22} \end{pmatrix}\begin{pmatrix} u_{\mathrm{s}}(z) \\ u_{\mathrm{as}}^{*}(z) \end{pmatrix} \quad (6)$$

with

$$\begin{aligned} a_{11} &= A(\Omega) + \gamma P_{\mathrm{p}}\left[(1-\xi)R(\Omega) - \xi R(0)\right], \\ a_{12} &= \gamma P_{\mathrm{p}}(1-\xi)R(\Omega), \\ a_{21} &= -\gamma P_{\mathrm{p}}(1+\xi)R(\Omega), \\ a_{22} &= B(\Omega) - \gamma P_{\mathrm{p}}\left[(1+\xi)R(\Omega) + \xi R(0)\right], \end{aligned}$$

and

$$\begin{aligned} A(\Omega) &= \sum_{n\geq 2}\frac{(-1)^n}{n!}\cdot\beta_n\cdot\Omega^n, \\ B(\Omega) &= \sum_{n\geq 2}\frac{(-1)}{n!}\cdot\beta_n\cdot\Omega^n, \end{aligned}$$

here $\xi = \Omega/\omega_{\mathrm{p}}$.

Suppose a solution of the type $u_{\mathrm{s}}(z)$ and $u_{\mathrm{as}}^{*}(z) \propto \exp(-\mathrm{i}\mu_{\pm}z)$ of Eq.(6). One easily finds the complex eigenvalue $\mu_{\pm} = \mu_{\mathrm{R}} + \mathrm{i}\mu_{\mathrm{I}}$ by calculating the roots of a second-order characteristic polynomial, which is determined by the following equation,

$$\begin{aligned} \mu_{\pm} = & C(\Omega) + \gamma P_{\mathrm{p}}\xi\left[R(\Omega) + R(0)\right] \\ & \pm \left[D(\Omega)^2 + 2\gamma P_{\mathrm{p}} R(\Omega) D(\Omega)\right. \\ & \left. + \gamma^2 P_{\mathrm{p}}^2 \xi^2 R^2(\Omega)\right]^{1/2} \end{aligned} \quad (7)$$

with

$$C(\Omega) = \sum_{n\geq 1}\frac{1}{(2n+1)!}\beta_{2n+1}\Omega^{2n+1},$$

$$D(\Omega) = \sum_{n\geq 1}\frac{1}{(2n)!}\beta_{2n}\Omega^{2n}.$$

Modulation instability occurs at the detuning frequency Ω, where the Stokes wave or anti-Stokes wave undergoes exponential growth when the MI gain coefficient is defined as $g_{\mathrm{MI}}(\Omega) = 2\mathrm{Im}(\mu_{\pm}) > 0$. Here $C(\Omega)$ and $R(0)$ are real numbers, so we can gain from Eq.(7)

$$\begin{aligned} g_{\mathrm{MI}}(\Omega) = & \ 2\ \mathrm{Im}\left\{\gamma P_{\mathrm{p}}\xi R(\Omega)\right. \\ & \pm \left[D(\Omega)^2 + 2\gamma P_{\mathrm{p}} R(\Omega) D(\Omega)\right. \\ & \left.\left. + \gamma^2 P_{\mathrm{p}}^2 \xi^2 R^2(\Omega)\right]^{1/2}\right\}. \end{aligned} \quad (8)$$

The requirement for the gain is the expression in the square root of Eq.(8) to satisfy the relation

$$\begin{aligned} & D(\Omega)^2 + 2\gamma P_{\mathrm{p}} R(\Omega) D(\Omega) \\ & \quad + \gamma^2 P_{\mathrm{p}}^2 \xi^2 R^2(\Omega) < 0. \end{aligned} \quad (9)$$

Thus, $D(\Omega)$ satisfies

$$\begin{aligned} & -\gamma P_{\mathrm{p}} R(\Omega)\left[1 + \sqrt{1-\xi^2}\right] < D(\Omega) \\ & \quad < -\gamma P_{\mathrm{p}} R(\Omega)\left[1 - \sqrt{1-\xi^2}\right]. \end{aligned}$$

Furthermore, assuming $g_{\mathrm{MI}}(\Omega) = 0$, we can attain the maximum gain bandwidth, which can be approximately expressed as

$$\begin{aligned} B_{\mathrm{MI}}^{\max} &\approx \Omega_{\max} \\ &\approx \sqrt{-12\beta_2/\beta_4}, \quad (\beta_2 < 0, \beta_4 > 0). \end{aligned} \quad (10)$$

Obviously, equations (8) and (9) indicate that MI gain depends on the nonlinear parameter γ and even-order dispersion coefficient β_{2n} of PCF (notice that the odd-order dispersion coefficient β_{2n+1} has no effect on MI) whereas γ and β_{2n} depend on the fibre structural parameters such as the air-hole diameter d and the pitch Λ between the holes. As a result, we can control the MI gain and its bandwidth by designing different PCF. Also, MI occurs not only in the anomalous GVD regime but also in the normal GVD regime when equation (9) is satisfied for a certain fibre.

4. Design of different structural PCFs with TZDWs for MI gain control

Based on the former description, we know that γ is inversely proportional to A_{eff}, which depends on the fibre structural parameters. Commonly, $A_{\mathrm{eff}} =$

$\pi r_{\rm eff}^2$ and $r_{\rm eff}$ is the effective waveguide mode radius of the fibre which can be described roughly by the formula[19,20]

$$r_{\rm eff} = r_{\rm c}(d, \Lambda, \lambda_{\rm p}) + \lambda_{\rm p}/\left[2\pi(n_{\rm c}^2\cos\phi - n_{\rm cl,eff}^2)^{1/2}\right], \quad (11)$$

where $r_{\rm c}$ is the fibre effective core radius which is related to the pump wavelength $\lambda_{\rm p}$ and the air-hole diameter d and the pitch Λ of PCF; $n_{\rm c}$ is the refractive index of the fibre core; ϕ is the incidence angle characterizing the mode in the fibre core; and $n_{\rm cl,eff}$ is the effective refractive index of the cladding, which depends on the fundamental space-filling mode EH_{11} of PCF cladding.

We may adopt the improved full vector index method (FVIM) to find $n_{\rm cl,eff}$. For this, we solve the characteristic equation of space-filling mode EH_{11} of fibre cladding in a circular unit cell with symmetric boundary conditions $\partial\psi/\partial s = 0$, where ψ is the electric field and s is the coordinate along the axis oriented in the direction perpendicular to the boundary of the unit cell. The characteristic equation of space-filling mode EH_{11} can be expressed as[21]

$$\frac{\mathrm{I}_2(wr)}{\mathrm{I}_1(wr)} + \frac{1}{wr} + \frac{wr}{2}\left(1 + \frac{n_{\rm co}^2}{n_{\rm air}^2}\right) g(u) + wr\left[\frac{1}{4}\left(1 - \frac{n_{\rm co}^2}{n_{\rm air}^2}\right)^2 g^2(u) + \frac{f(w,u)}{n_{\rm air}^2}\right]^{1/2} = 0 \quad (12)$$

with

$$g(u) = \frac{1}{ur}\frac{\mathrm{J}_0(ur)\mathrm{Y}_1(uR) - \mathrm{Y}_0(ur)\mathrm{J}_1(uR)}{\mathrm{J}_1(ur)\mathrm{Y}_1(uR) - \mathrm{Y}_1(ur)\mathrm{J}_1(uR)} - \frac{1}{u^2r^2},$$
$$f(w,u) = \frac{1}{r^4}\left(\frac{1}{u^2} + \frac{1}{w^2}\right)\left(\frac{n_{\rm co}^2}{u^2} + \frac{n_{\rm air}^2}{w^2}\right),$$

and

$$w^2 = \omega^2\left(n_{\rm cl,eff}^2 - n_{\rm air}^2\right)/c^2,$$
$$u^2 = \omega^2\left(n_{\rm co}^2 - n_{\rm cl,eff}^2\right)/c^2,$$

where I, J and Y are Bessel functions, r and R are the air-hole radius and the equivalent circular unit cell radius of the PCF, respectively; $n_{\rm air}$ and $n_{\rm co}$ are the refractive index of air and quartz medium, respectively. Considering the material dispersion, $n_{\rm co}$ is well approximated by the Sellmeier equation. Therefore, by numerically solving Eq.(12), we can have $u = u(\omega)$, and then obtain

$$n_{\rm cl,eff}(\omega) = \sqrt{n_{\rm co}^2 - u^2(\omega)\,c^2/\omega^2}. \quad (13)$$

With $n_{\rm cl,eff}$, the effective refractive index $n_{\rm eff}$ of the fundamental mode HE_{11} transmitted in the fibre can be attained by solving the following characteristic equation[21]

$$\frac{J_0(U)}{J_1(U)} = \frac{1}{U} + \frac{U}{2}\left(1 + \frac{n_{\rm cl,eff}^2}{n_{\rm co}^2}\right)\left[\frac{1}{W^2} + \frac{K_0(W)}{W\cdot K_1(W)}\right] - \frac{U}{2}\sqrt{\left(1 - \frac{n_{\rm cl,eff}^2}{n_{\rm co}^2}\right)^2\left[\frac{1}{W^2} + \frac{K_0(W)}{W\cdot K_1(W)}\right]^2 + 4F(U,W)} \quad (14)$$

with

$$F(U,W) = \left[\frac{1}{U^2} + \frac{1}{W^2}\right]\left[\frac{1}{U^2} + \frac{n_{\rm cl,eff}^2}{n_{\rm co}^2}\cdot\frac{1}{W^2}\right]$$

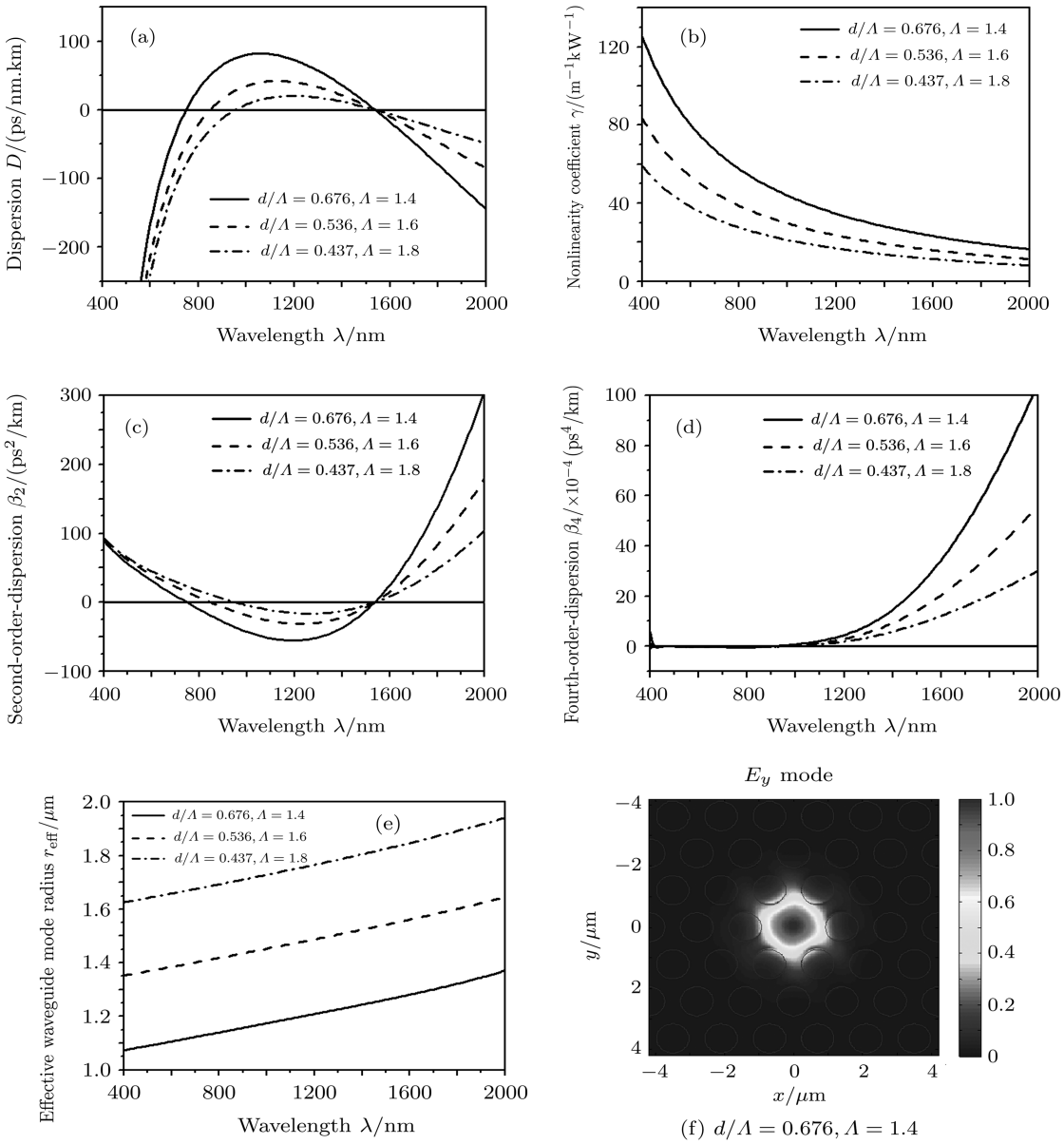
and

$$U^2 = k_0^2(n_{\rm co}^2 - n_{\rm eff}^2)\cdot r_{\rm c}^2,$$
$$W^2 = k_0^2(n_{\rm eff}^2 - n_{\rm cl,eff}^2)\cdot r_{\rm c}^2,$$

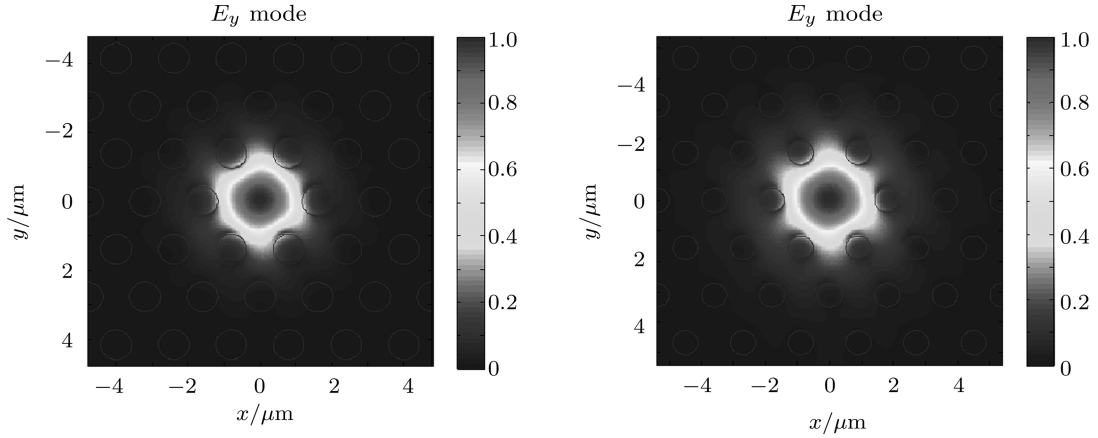
where k_0 is the free space wave number. Finally, making use of the dispersion parameter $D(\omega) = -(\lambda/c)(\mathrm{d}^2 n_{\rm eff}(\omega)/\mathrm{d}\lambda^2) = -(2\pi c/\lambda^2)k_2(\omega)$, the other high-order dispersion coefficients can be also acquired, $k_2(\omega) = \sum_{n\geq 2}(\beta_n/(n-2)!)\,\Omega^{n-2}$, with $k_2(\omega)$ being the frequency-dependent dispersion.

For conveniently studying the effect of the fibre structure on MI gain in the following sections, we design three types of PCFs with two ZDWs. Figure 1(a) shows the dispersion property of PCFs with different parameters d/Λ. Figure 1(e) gives the variation of the effective waveguide mode radius $r_{\rm eff}$ with the wavelength for different parameters d/Λ, indicating that $r_{\rm eff}$ gradually increases with the increase of d/Λ and λ. Figure 1(f), 1(g) and 1(h) show the field plots of the y-polarization fundamental mode for pump wavelength $\lambda_{\rm p} = 1530$ nm, which can be attained by using the FDFD method to numerically solve the Maxwell equation.[22] As can be seen, the first ZDWs are dif-

ferent from each other while the second ZDWs are the same and equal to $\lambda_p = 1530$ nm. Besides the pump power, pump wavelength and Raman gain, equation (8) indicates that MI gain also depends mainly on the even-order dispersion coefficients β_{2n} and the nonlinear parameter γ of the fibre. Here, the variation of the second, fourth-order dispersion coefficients with wavelength is given by Figs.1(c) and 1(d), respectively. Meanwhile, the nonlinear parameter γ is also shown in Fig.1(b). Figure 1(d) implies that, for visible wavelengths, the fourth-order dispersion coefficients are almost equal to 0. Hence, it is unnecessary to discuss the effect of high-order dispersion on MI gain if the pump wavelength is close to the first ZDWs. As a result, the pump wavelength should be chosen not only close to the second ZDW 1538 nm but also slightly less than 1538 nm, so as to ensure $\beta_2 < 0$. The other even-order dispersions β_{2n} $(n \geq 3)$, such as $\beta_6 = 6.3 \times 10^{-8}$ ps^8/km of the fibre with $d/\Lambda = 0.676$ and $\Lambda = 1.4$ μm, have almost no impact on the MI gain due to the very small dispersion values even if the pump wavelength lies in the infrared light region, so they can be neglected. Therefore, it is interesting and necessary to investigate the detailed behaviour of the fourth-order dispersion on MI gain for PCFs with different structural parameters when the pump wavelength is close to the second ZDW.



(f) $d/\Lambda = 0.676, \Lambda = 1.4$



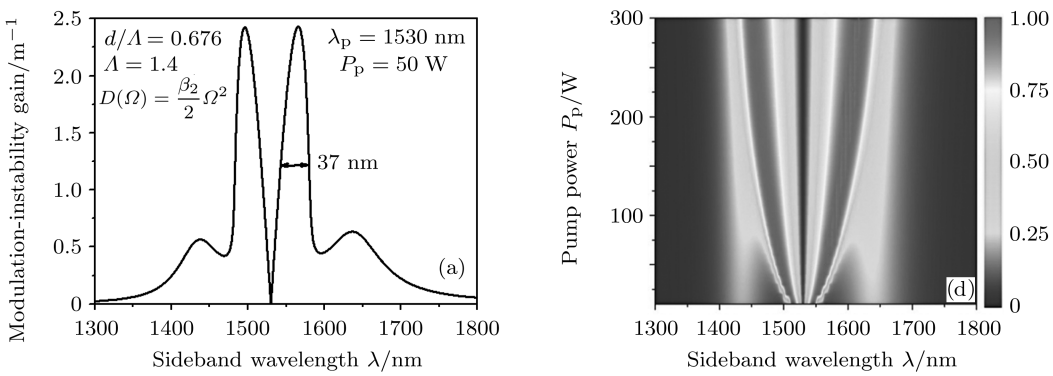
(g) $d/\Lambda = 0.536, \Lambda = 1.6$ (h) $d/\Lambda = 0.437, \Lambda = 1.8$

Fig.1. (a) and (b) are the calculated dispersion coefficient and nonlinear parameter variation with wavelength, respectively. (c) and (d) are the second-order and fourth-order dispersions of the fibre, respectively. (e) is the variation of the effective waveguide mode radius with wavelength. (f), (g) and (h) are the calculated field plots of the y-polarization fundamental mode for different fibres with TZDWs at pump wavelength $\lambda_{\rm p} = 1530$ nm.

5. Effect of fibre structure, pump power and wavelength on MI gain

Figures 2(a), 2(b) and 2(c) show the MI gain variation with sideband wavelengths for PCF with $d/\Lambda = 0.676$, $\Lambda = 1.4$ μm, $\beta_2 = -3.0693$ ps^2/km and $\beta_4 = 2.6205 \times 10^{-3}$ ps^4/km when $\lambda_{\rm p} = 1530$ nm and $P_{\rm p} = 50$ W. Defining the full width at half maximum (FWHM) of the MI gain peak as gain bandwidth, we see from Figs.2(a) and 2(c) that the presence of the positive FOD not only leads to generation of two extra MI gain peaks but also a fourfold increase in MI gain bandwidth, from 37 nm to 148 nm, which is not so flat due to the low pump power. This case illustrates that the short-wave gain peak at the anti-Stokes sideband is associated with the usual MI owing to the negative GVD of the fibre, whereas the long-wave gain peak depends on the positive FOD and is located at the sideband detuning $\Omega_{\max}/(2\pi) \cong \sqrt{-12\beta_2/\beta_4}/(2\pi) = 18.6$ THz, which corresponds to a sideband shift of ∼140 nm. It should be mentioned that the combination of GVD and FOD is not optimal here, although it will be optimized in Figs.4 and 5.

The detailed dependence of the MI gain upon the pump power and the sideband wavelength detuning from the pump wavelength is shown in Figs.2(d), 2(e) and 2(f). To better express the MI gain magnitude, we use a bar to represent the normalized MI gain value. Analysing Figs.2(d), 2(e) and 2(f), we find that the flat-top MI gain profile certainly depends on the pump power, and the gain bandwidth gradually increases with augmentation of the pump power. If we just consider the effect of GVD or FOD on MI gain, a two-peak profile at the anti-Stokes sideband or Stokes sideband does not exist for any pump power (see Figs.2(d) and 2(e)).



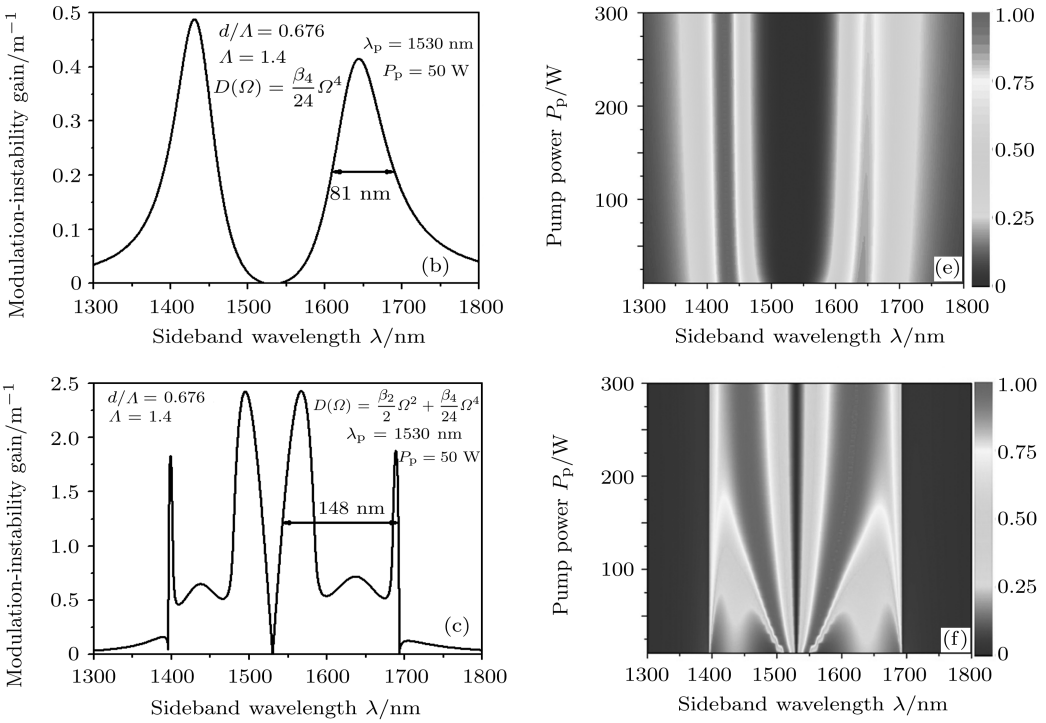


Fig.2. (a), (b) and (c) show the MI gain variation with sideband wavelength for pump power $P_p = 50$ W. (d), (e) and (f) are the sideband wavelength variation with different powers. (a) and (d) only consider the effect of GVD β_2. (b) and (e) only consider the effect of FOD β_4. (c) and (f) consider the combined effect of GVD β_2 and FOD β_4. A bar showing the normalized MI gain values is given on the right side of each of parts (d), (e) and (f).

Conversely, if the corporate effect of GVD and FOD on MI gain is considered, a great change occurs obviously. For $P_p < 175$ W, a two-peak gain profile appears at the anti-Stokes sideband or Stokes sideband (see Fig.2(f)), but they have different gain magnitudes (see Fig.2(c)); the gain value at 1567 nm is 1.3 times that at 1688 nm. But, if $P_p > 175$ W, the two gain peaks merge together into a single broadband gain profile at the anti-Stokes sideband or Stokes sideband (see Fig.2(f)). Thus, we can control the broadband MI gain magnitude and its gain profile by choosing an appropriate pump power when the pump wavelength is below the second ZDW λ_{z2}. Moreover, we can also decrease the MI gain magnitude and its bandwidth by reducing the pump power and compensating GVD. Comparing Fig.2(b) with 2(c), we discover that GVD compensation gives the maximum gain and its bandwidth decreases by $\sim 4/5$ and $\sim 9/20$ for $P_p = 50$ W, respectively.

Although the MI gain and its bandwidth depend on the pump power of the incident pulse, the gain bandwidth mainly depends on the fibre structural parameters d/Λ because different structural parameters are linked to different dispersion values, especially GVD and FOD, which severely affect the MI gain bandwidth and gain profile. Figure 3 shows the MI gain profile of three fibres of different structures at pump power $P_p = 200$ W. In Fig.3(a), when only the effect of GVD is considered, the MI gain bandwidth for the fibre with $d/\Lambda = 0.437$ and $\Lambda = 1.8$ μm is maximal and equal to 92 nm, whereas the MI gain bandwidth for the fibre with $d/\Lambda = 0.676$ and $\Lambda = 1.4$ μm is minimal and equal to 80 nm. But their peak gain amplitudes are the reverse of each other: the former's peak gain amplitude is about half of the latter's peak gain amplitude, one is 4.8 m^{-1} and the other is 9.7 m^{-1}. If the corporate operation of GVD and FOD is considered in Fig.3(b), the MI gain bandwidths of the three fibres will all increase to above 110 nm and their peak gain amplitudes are not affected by the introduction of FOD. Comparing Fig.3(a) with Fig.3(b), we see that the gain bandwidths of the three PCFs are 80 nm, 86 nm and 92 nm respectively with $D(\Omega) = \beta_2\Omega^2/2$, while with $D(\Omega) = \beta_2\Omega^2/2 + \beta_4\Omega^4/24$ their MI gain bandwidths are 132 nm, 125 nm and 115 nm respectively. Their increments are 52 nm, 39 nm and 23 nm, respectively. This case illustrates that the effect of FOD on the MI gain bandwidth of fibres with larger

d/Λ is much larger than those with smaller d/Λ. Furthermore, different pump powers and fibre parameters lead to different gain flatness. In Fig.3(b), the gain flatness for the fibre with $d/\Lambda = 0.676$ and $\Lambda = 1.4$ μm is the best among the designed three PCFs, which implies that MI gain peaks can become much flatter if an appropriate pump power is chosen. Therefore, by designing an appropriate fibre parameter d/Λ and controlling the pump power, we can obtain ultra-broadband and flat-top MI gain room, which is important to obtaining broadband amplification using optical fibres, and may be a worthwhile and hopeful amplification technology in the future.

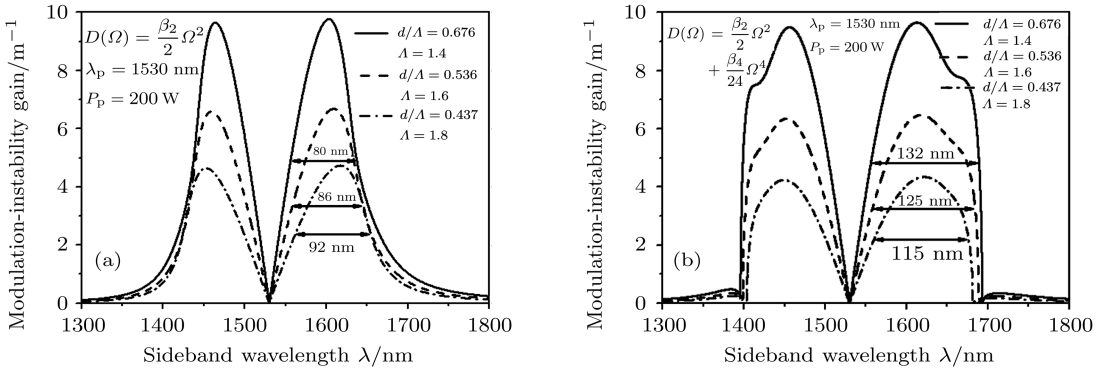


Fig.3. Comparison of MI gain bandwidth variations for three fibres of different structures. (a) MI gain for $D(\Omega) = \frac{\beta_2}{2}\Omega^2$, (b) MI gain for $D(\Omega) = \frac{\beta_2}{2}\Omega^2 + \frac{\beta_4}{24}\Omega^4$.

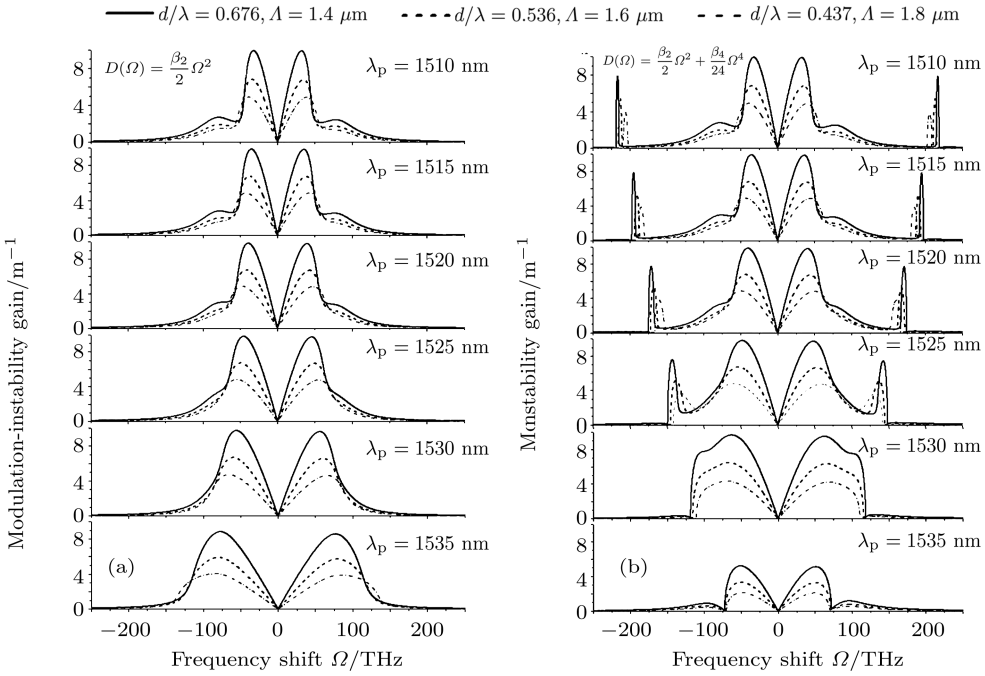


Fig.4. MI gain variation of three different fibres with different frequency shifts for pump power $P_p = 200$ W. (a) MI gain for $D(\Omega) = \frac{\beta_2}{2}\Omega^2$, (b) MI gain for $D(\Omega) = \frac{\beta_2}{2}\Omega^2 + \frac{\beta_4}{24}\Omega^4$.

Besides pump power and fibre structural parameters, the pump wavelength is also an important factor in MI gain. Figure 4 shows the MI gain variation with different pump wavelengths at $P_p = 200$ W. In view of Fig.4, when GVD and FOD work simultaneously and the pump power remains constant, the MI gain bandwidth of the three different fibres gradually decreases as pump wavelength increases, while their gain flatness gradually becomes smooth. Moreover, there exists an optimal pump wavelength region close to $\lambda_p = 1530$ nm,

corresponding to about 8 nm of downshift from the fibres' ZDW $\lambda_{z2} = 1538$ nm. However, if FOD can be compensated by a grating pair or another method, the optimal pump wavelength region should be close to $\lambda_{z2} = 1538$ nm, for example, $\lambda_{\rm p} = 1535$ nm as shown in Fig.4(a). Therefore, to obtain a flat-top gain profile and a much higher gain magnitude, it is necessary to choose the optimal pump wavelength for any fibre.

6. Optimal control of MI gain

Based on the above analysis, in order to achieve the optimal gain design, it is better to choose the optimal fibre parameter $\Lambda = 1.4$ μm and $d/\Lambda = 0.676$ among the three designed PCFs. Moreover, the pump power should be > 175 W and the pump wavelength should be limited to a small region close to 1530 nm. Figure 5(a) shows the MI gain profile versus sideband wavelength for five different pump wavelengths in a small region close to 1530 nm at pump power $P_{\rm p} = 250$ W. The comparisons display that the optimal pump wavelength is just $\lambda_{\rm p}^{\rm opt} = 1530$ nm and the optimal gain bandwidth is ~130 nm which is less than the maximal gain bandwidth 140 nm obtained from the formula $B_{\rm MI}^{\rm max} \approx \Omega_{\rm max} \approx \sqrt{-12\beta_2/\beta_4}$. In the case of the optimal pump wavelength and the fibre parameter, the optimal nonlinearity $\gamma^{\rm opt}$ is given by $\gamma^{\rm opt} = n_2\omega_{\rm p}^{\rm opt}/cA_{\rm eff}^{\rm opt} = 2n_2/\lambda_{\rm p}^{\rm opt}(r_{\rm eff}^{\rm opt})^2$ and the optimal sideband detuning $\Omega_{\rm opt}^{\rm peak} \sim (5/8)\Omega_{\rm max}$ corresponding to MI peak gain can be obtained from Fig.5(a). Since the maximum MI gain is given by the phasing matching condition $D(\Omega_{\rm opt}^{\rm peak}) + \gamma^{\rm opt}P_{\rm p}^{\rm opt} = 0$ by neglecting the contribution of Raman gain, one obtains the optimal power design rules by using Eqs.(7) and (11), and only considering GVD and TOD:

$$P_{\rm p}^{\rm opt} = \frac{23}{16\gamma^{\rm opt}}\frac{\beta_2^2}{\beta_4}, \tag{15}$$

$$\gamma^{\rm opt} = 2n_2/\left\{\lambda_{\rm p}^{\rm opt}\left[r_{\rm c}(d,\Lambda,\lambda_{\rm p}^{\rm opt}) + \lambda_{\rm p}^{\rm opt}\Big/\left[2\pi\sqrt{n_{\rm c}^2\cos\varphi - n_{\rm cl,eff}^2}\,\right]\right]^2\right\}. \tag{16}$$

Obviously, the optimal pump power depends on the optimal fibre structure and optimal pump wavelength (see Eqs.(15) and (16)). The appropriate pump power is determined in the following way. Once the optimal fibre with TZDWs is chosen, we have its second ZDW value λ_{z2}. Then the optimal wavelength is certain to lie in about an 8 nm interval of downshift from λ_{z2} according to Fig.4. In succession, making use of formulas (15) and (16), the optimal pump power can be roughly estimated. Finally, by appropriately changing the estimated pump power value, the optimal pump power can be established. For example, for the designed fibre with $\Lambda = 1.4$ μm and $d/\Lambda = 0.676$, the estimated optimal pump power from formula (15) is 210 W, and we may change the pump power from 200 W to 300 W to ascertain the optimal pump power. In fact, from Fig.5(b), we see that, corresponding to the optimal pump wavelength $\lambda_{\rm p} = 1530$ nm, the pump power $P_{\rm p} = 250$ W is the optimal choice, which illustrates that using formula (15) to roughly evaluate the optimal pump power is credible. The difference is related to the choice of the optimal pump wavelength and the approximation of the fibre effective core radius.

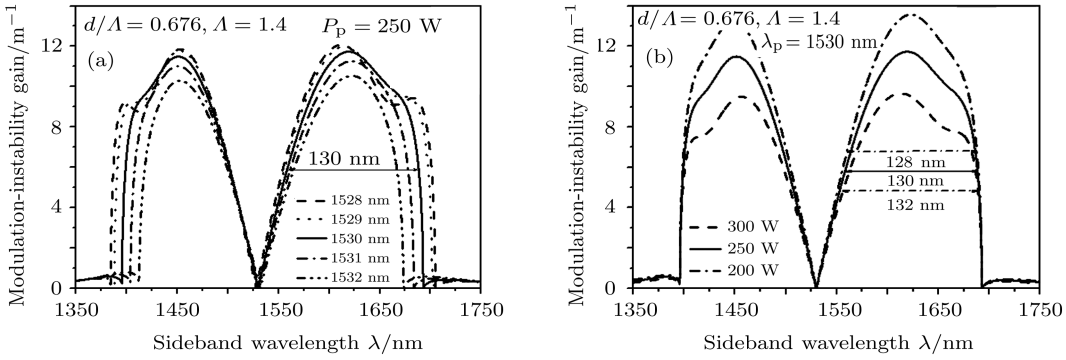


Fig.5. Optimal design of MI gains: (a) for different pump wavelengths at pump power $P_{\rm p} = 250$ W; (b) for different pump powers at pump wavelength $\lambda_{\rm p} = 1530$ nm.

Although there are some other methods to obtain optical amplification, such as optical parametric amplification and Raman amplification, they may have some disadvantages. Optical parametric amplification can be used to find a higher gain value, but its gain bandwidth is usually limited to about 100 nm. Raman amplification can be used to attain a wider gain bandwidth (40 THz), but its gain profile is not flat and can be described by a single-Lorentzian model. However, MI gain amplification, including the combined operation of parametric and Raman gain, has the merits of both optical parametric amplification and Raman amplification. It not only enhances the gain bandwidth of the fibre amplifier to 130 nm in the anti-Stokes region or Stokes region (total gain bandwidth is 260 nm) and attains a flat-top gain profile, but also results in a much higher gain value as compared with the Raman gain of the fibre. For example, a nearly four-fold gain increase has been experimentally observed in relatively recent experiments.[8] Thus, using the MI method to obtain better broadband and flat-top gain will be a promising amplification technique.

7. Conclusion

In this paper, we have designed three types of PCFs with TZDWs and different air hole diameter (d) to pitch (Λ) ratios d/Λ by improved FVIM and FDFD techniques. The first ZDWs are different and the second ZDWs are the same and equal to 1538 nm. The effect of pump power, incident wavelength and fibre structure on MI gain is comprehensively investigated. The results show that, with the increase of pump power and wavelength in the anomalous region close to the second ZDW 1538 nm, the two gain peaks at the anti-Stokes or Stokes sideband may merge together into a single broadband gain profile. Moreover, there exist both optimal pump wavelength and power, which depend on the fibre structure parameters. For the optimal fibre with parameter $d/\Lambda = 0.670$ and $\Lambda = 1.4$ μm the optimal pump wavelength is 1530 nm, which lies in an interval of about 8 nm of downshift from the second ZDW 1538 nm, and the optimal pump power is about 250 W. Based on the optimal fibre structure, optimal pump wavelength and power, an optimal MI gain bandwidth of 130 nm at the anti-Stokes or Stokes sideband is obtained. It is noted that the optimal pump wavelength and pump power vary with the second ZDW of the fibre. As a result, the MI gain bandwidth and flatness can be efficiently improved and controlled by appropriately designing the fibre structure and choosing the pump wavelength and power, which may be useful to the enhancement of amplifier gain and bandwidth. Conversely, restricting MI gain by compensating the GVD and FOD of the fibre is also useful in some special fields, such as long-haul optical communication systems.

References

[1] Harvey J D, Leonhardt R, Coen S, Wong G K L, Knight J C, Wadsworth W J and Russell P S J 2003 *Opt. Lett.* **28** 2225

[2] Wadsworth W J, Joly N, Knight J C, Birks T A, Biancalana F and Russel P St J 2004 *Opt. Express* **12** 299

[3] Akheelesh A K, Headley C and Jorgensen C G 2004 *Opt. Express* **29** 2163

[4] Agrawal G P 2001 *Nonlinear Fibre Optics* (Beijing: Academic Press) p136 (in Chinese)

[5] Tai K, Hasegawa A and Tomita A 1986 *Phys. Rev. Lett.* **56** 135

[6] Wen S C and Fan D Y 2002 *J. Opt. Soc. Am.* B **19** 1653

[7] Agrawal G P 1987 *Phys. Rev. Lett.* **59** 880

[8] Frédérique V, Philippe E and Stéphane C 2003 *Opt. Lett.* **28** 1960

[9] Hui R Q, Maurice O, Alan R and Mike T 1997 *Journal of Lightwave Technology* **15** 1071

[10] Dai X Y, Wen S C and Xiang Y J 2008 *Acta Phys. Sin.* **57** 186 (in Chinese)

[11] Ding W S, Xi L and Liu L H 2008 *Acta Phys. Sin.* **57** 7705 (in Chinese)

[12] Zhong X Q and Xiang A P 2007 *Chin. Phys.* **16** 1683

[13] Millot G, Saute R A, Provino L, Dudley J M and Windeler R W 2002 *Opt. Lett.* **27** 695

[14] Marhic M E, Kagi N, Chiang T K and Kazovsky L G 1996 *Opt. Lett.* **21** 573

[15] Zhang A L and Demokan M S 2004 *Opt. Lett.* **30** 2375

[16] Wang Y, Zhang W, Wang Q, Feng X, Liu X M and Peng J D 2004 *Opt. Lett.* **29** 842

[17] Matos C J S de, Taylor J R and Hansen K P 2004 *Opt. Lett.* **29** 983

[18] Lin Q and Agrawal G P 2006 *Opt. Lett.* **31** 3086

[19] Fedotov A B, Naumov A N and Zheltikov A M 2002 *J. Opt. Soc. Am.* B **19** 2156

[20] Li Y F, Yao Y H, Hu M L, Chai L and Wang C Y 2008 *Appl. Opt.* **47** 399

[21] Li Y F, Wang C Y and Hu M L 2004 *Opt. Commun.* **238** 29

[22] Zhu Z M and Brown T G 2002 *Opt. Express* **10** 853